

# The d1g(v=1) Rydberg state of O2: Optical-optical double-resonance and Huggins-band ozone-photolysis, resonance-enhanced multiphoton-ionization studies with a b1+g(v=0)-state platform



# The d 1 Π g (v=1) Rydberg state of O 2 : Optical-optical double-resonance and Huggins-band ozone-photolysis, resonance-enhanced multiphoton-ionization studies with a b 1 Σ g + (v=0) -state platform

P. O'Keeffe, T. Ridley, H. A. Sheard, K. P. Lawley, R. J. Donovan, and B. R. Lewis

Citation: The Journal of Chemical Physics **117**, 8705 (2002); doi: 10.1063/1.1513462
View online: http://dx.doi.org/10.1063/1.1513462
View Table of Contents: http://scitation.aip.org/content/aip/journal/jcp/117/19?ver=pdfcov
Published by the AIP Publishing

# The $d\,^1\Pi_g(v=1)$ Rydberg state of $O_2$: Optical-optical double-resonance and Huggins-band ozone-photolysis, resonance-enhanced multiphoton-ionization studies with a $b\,^1\Sigma_g^+(v=0)$-state platform

P. O'Keeffe,[a] T. Ridley, H. A. Sheard, K. P. Lawley, and R. J. Donovan
*Department of Chemistry, The University of Edinburgh, West Mains Road, Edinburgh, EH9 3JJ, Scotland*

B. R. Lewis
*Research School of Physical Sciences and Engineering, The Australian National University, Canberra, ACT 0200, Australia*

(Received 7 May 2002; accepted 20 August 2002)

Resonance-enhanced multiphoton-ionization spectra are presented of the $d\,^1\Pi_g \leftarrow\leftarrow b\,^1\Sigma_g^+(1,0)$ transition of $O_2$, the $b(v=0)$ state generated both by photolysis of $O_3$ in the Huggins bands and also by direct excitation of single $J$ levels in an optical-optical double-resonance (OODR) experiment. The ozone-photolysis-derived spectra reveal a preferential formation of $b(v=0)$ fragments with high $J$, the rotational distributions exhibiting significant dependence on the photolysis wavelength. Rotational analyses of the OODR and ozone-photolysis-derived spectra indicate that the $d(v=1)$ Rydberg state is multiply perturbed by successive vibrational levels of the $II\,^1\Pi_g$ valence state. The OODR technique allows the first full resolution of the low-$J$ levels of $d(v=1)$ and the high-$J$ levels favored by the ozone-photolysis technique are reported here for the first time. © *2002 American Institute of Physics.* [DOI: 10.1063/1.1513462]

The $d\,^1\Pi_g$ Rydberg state of $O_2$ has been the subject of renewed interest, not only fundamentally, due to its complex spectroscopy,[1,2] but also through its use as an intermediate state in resonance-enhanced multiphoton-ionization (REMPI) dynamical probes of the metastable singlet states, $a\,^1\Delta_g$ and $b\,^1\Sigma_g^+$, formed by microwave[3] or optical[3–6] excitation of $O_2$, or photolysis of $O_3$.[3,7]

Two of these experimental techniques have recently provided advances in knowledge of the $d$-state spectroscopy, particularly through the use of the $b$ state as a platform. First, optical-optical double-resonance (OODR)-REMPI studies have been performed on the $d(v=0)$[6] and $d(v=3)$[5] levels excited *via* single rotational levels of the $b(v=0)$ state, resulting in great spectral simplification and full resolution of many rotational levels for the first time, together with the revelation of local perturbations[5] and unique quantum-interference effects.[8] Second, the REMPI probing of ozone-photolysis products has provided the first information on high rotational levels of $d(v=2-4)$, as well as interesting dynamical information on the formation of $O_2(a\,^1\Delta_g)$ and, of most relevance to this work, $O_2(b\,^1\Sigma_g^+)$ in the photodissociation of ozone.[3,7] In particular, O'Keeffe *et al.*[7] have demonstrated the production of $O_2(b\,^1\Sigma_g^+)$ following the photolysis of $O_3$ in the Huggins bands,

$$O_3 + h\nu(\lambda_{\text{thresh}} = 463\ \text{nm}) \rightarrow O(^3P_J) + O_2(b\,^1\Sigma_g^+), \quad (1)$$

by observing the $d\leftarrow\leftarrow b(2,0)$ transition in a $(2+1)$-REMPI probe of the $O_2$ photofragments. However, they[7] were unable to quantify the nascent $J$ distribution of the $b(v=0)$ fragments because of strong perturbation of the $d(v=2)$ level due to Rydberg-valence interactions.[1]

Here, we report observations of the $d\leftarrow\leftarrow b(1,0)$ band of $O_2$ following Huggins-band photolysis of $O_3$. Analyses of these REMPI spectra yield, not only the first information on $d(v=1)$ rotational levels with $J>29$, including the revelation of a series of Rydberg-valence perturbations, but also the first estimate of an $O_2(b)$-state fragment rotational distribution in $O_3$ photolysis, which is found to peak at high $J$. These data are supported by an OODR-REMPI study of the $J=1-18$ levels of $d(v=1)$ which has allowed their full resolution for the first time. The only previous rotational analyses for $d(v=1)$, from $d\leftarrow\leftarrow a(1,0)$ and/or $d\leftarrow\leftarrow X(1,0)$ spectra[9,10] containing many blended lines, are those of Sur *et al.*[9] $(J=1-12)$ and Lewis *et al.*[2] $(J=1-29)$.

The apparatus for the ozone photolysis experiment has been described elsewhere.[7] Briefly, independently tunable, counterpropagating, XeCl-excimer-pumped, dye-laser pump (PTP, 10 mJ per pulse) and probe (QUI, 20 mJ per pulse) beams were focused together simultaneously, using lenses of 6 cm focal length, in an ionization chamber, intersecting a pulsed $O_3$-in-He molecular beam at 90°. Following photolysis of the ozone by the pump beam, the resultant $O_2[b\,^1\Sigma_g^+(v=0)]$ fragments were probed using a $[(1+1')+1]$-REMPI scheme, accessing the $d(v=1)$ state at the two-photon step. The $O_2^+$ ions produced were collected by a linear time-of-flight mass spectrometer and the ion current from the micro-channel-plate detector was processed by a boxcar integrator. The very similar apparatus for the OODR experiment has also been described elsewhere.[6] In this case, a pulsed $O_2$ molecular beam was employed and the pump laser (R700, 5 mJ per pulse) was used to directly pump the

[a]Present address: LURE, Bâtiment 209D, Center Universitaire Paris-Sud, F-91898, Orsay Cedex, France.

 

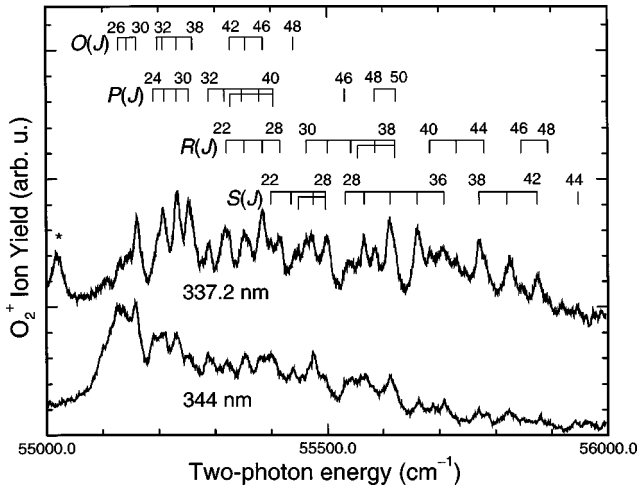


FIG. 1. $[(1+1')+1]$-REMPI spectra for the $d\,^1\Pi_g \leftarrow\leftarrow b\,^1\Sigma_g^+(1,0)$ band of $O_2$, obtained following photodissociation of $O_3$ in the Huggins bands at 337.2 and 344.0 nm, together with rotational assignments. The peak marked with an asterisk results from a $[(1+2')+1]$-REMPI process and is not associated with the *d* state.

$b\,^1\Sigma_g^+ \leftarrow X\,^3\Sigma_g^-(0,0)$ magnetic-dipole transition of $O_2$ near 760 nm, selectively exciting single rotational levels of the *b* state. These levels were probed (frequency-doubled C102, 3 mJ per pulse) using a $[(1+1')+1']$-REMPI scheme.

In the OODR experiment, the probe laser was simultaneously calibrated optogalvanically,[6] while the accurately known $b \leftarrow X$ transition energies[11] served to effectively calibrate the pump laser. As a result, the OODR spectra are, in principle, calibrated to $\pm 0.5$ $cm^{-1}$. However, we note that Ridley *et al.*,[6] in a comparable OODR study of the $d(v=0)$ state, found that the line positions were subject to laser-power-dependent shifts of up to 2 $cm^{-1}$ to the blue, so the current spectra may be subject to an additional systematic energy uncertainty. Unfortunately, since maximum laser power was normally necessary to obtain spectra of reasonable signal-to-noise ratio for transitions to these strongly predissociated $d(v=1)$ levels,[2] it was not possible to perform meaningful power-dependence studies of the line positions and widths in either the ozone-photolysis or OODR experiments. The ozone-photolysis-derived spectra were calibrated against the OODR spectra, indirectly, by comparing the corresponding inferred $d(v=1)$ term values. Since, as will be seen below, different groups of *d*-state rotational levels were probed in each experiment, some degree of extrapolation was involved in this procedure. The additional uncertainty introduced by this extrapolation was minimized by bridging the gap between each set of measurements using the *relative* $d(v=1)$ terms of Lewis *et al.*[2] We estimate that the resultant absolute calibration uncertainty for the ozone-photolysis-derived spectra is $\pm 2$ $cm^{-1}$.

The $d \leftarrow\leftarrow b(1,0)$ $[(1+1')+1]$-REMPI spectra recorded following $O_3$ photolysis at 337.2 and 344 nm, shown in Fig. 1, exhibit regions of perturbation and differ significantly, suggesting photolysis-wavelength-dependent *J* distributions for the $b(v=0)$ fragments, higher *J*-values corresponding to the shorter photolysis wavelength. The spectra are significantly power broadened, with apparent line widths of $\sim 8$ $cm^{-1}$ full-width at half-maximum (FWHM). Nevertheless, we have managed to assign most of the rotational structure, which, as indicated in Fig. 1, appears to originate preferentially from *b*-state rotational levels in the range $J=22-50$. Transition energies for the rotational branches assigned in Fig. 1, listed in the second part of Table I, were determined from the positions of peaks in the two spectra.[12] Many lines are either partially or completely blended, but the *S*-branch peaks are fairly well resolved. The estimated uncertainty in determining the energy of an isolated peak is $\sim 1$ $cm^{-1}$, i.e., less than the absolute calibration uncertainty.

TABLE I. Rotational-branch energies for $d\,^1\Pi_g(v=1) \leftarrow\leftarrow b\,^1\Sigma_g^+(v=0,J)$ transitions observed in the REMPI spectrum of $O_2$, in $cm^{-1}$. For $J \leqslant 16$, the energies are from the OODR spectra of Fig. 2; for $J \geqslant 22$, the energies are from the ozone-photolysis-derived spectra of Fig. 1. Due to perturbations, the transitions are grouped in five segments, *a* through *e* (see text).

| $J$ | $O_a(J)$ | $P_a(J)$ | $R_a(J)$ | $S_a(J)$ |
|---|---|---|---|---|
| 0 | | | | 55 117.7 |
| 2 | | 55 103.7 | 55 119.3 | 55 131.9 |
| 4 | 55 090.5 | 55 100.6 | 55 129.6 | 55 149.0 |
| 6 | 55 082.3 | 55 100.3 | 55 140.8 | 55 168.1 |
| 8 | 55 077.3 | 55 100.4 | 55 155.5 | 55 187.7 |
| 10 | 55 074.0 | 55 102.7 | 55 168.4 | |
| 12 | 55 071.0 | 55 106.4 | | |
| | $O_b(J)$ | $P_b(J)$ | $R_b(J)$ | $S_b(J)$ |
| 12 | | | | 55 245.2 |
| 14 | | | 55 218.8 | 55 270.7 |
| 16 | 55 083.4 | 55 132.8 | 55 240.3 | 55 298.9 |
| 22 | | | 55 320.2 | 55 399.6 |
| 24 | | 55 190.5[a] | 55 353.8[b] | 55 438.5 |
| 26 | 55 128.6[a] | 55 209.7[a] | 55 384.4[b] | 55 475.1 |
| 28 | 55 142.7[a] | 55 231.7[b] | 55 416.1 | 55 497.5[a] |
| 30 | 55 159.7[b] | 55 253.0 | | 55 448.6 |
| 32 | 55 159.7[b] | | | |
| | $O_c(J)$ | $P_c(J)$ | $R_c(J)$ | $S_c(J)$ |
| 28 | | | | 55 532.9[a] |
| 30 | | | 55 462.5 | 55 566.3 |
| 32 | 55 196.9[a] | 55 288.6 | 55 500.9[a] | 55 612.5 |
| 34 | 55 206.9 | 55 316.0[a] | 55 542.8 | 55 661.7 |
| 36 | 55 231.7[b] | 55 347.3[a] | 55 585.6[b] | 55 708.7 |
| 38 | 55 259.8[a] | 55 378.7[a] | 55 622.9[a,b] | |
| 40 | | 55 405.7[a] | 55 555.3[a] | |
| 42 | | 55 326.4[a,b] | | |
| | $O_d(J)$ | $P_d(J)$ | $R_d(J)$ | $S_d(J)$ |
| 38 | | | | 55 771.1 |
| 40 | | | 55 684.0 | 55 820.2 |
| 42 | 55 326.4[a,b] | | 55 730.6 | 55 875.1 |
| 44 | 55 353.8[b] | | 55 780.3[a] | |
| 46 | 55 384.4[b] | 55 531.3[a] | | |
| | $O_e(J)$ | $P_e(J)$ | $R_e(J)$ | $S_e(J)$ |
| 44 | | | | 55 948.0 |
| 46 | | | 55 846.2[a] | |
| 48 | 55 439.6[a] | 55 585.6[b] | 55 893.8[a] | |
| 50 | | 55 622.9[a,b] | | |

[a]Shoulder.
[b]Blended.

The $d(v=1,J_d)\leftarrow\leftarrow b(v=0,J_b)$ OODR-[$(1+1')+1'$]-REMPI spectra are shown in Fig. 2 for $J_b=0-16$. Each spectrum in Fig. 2 has been shifted upwards in energy by an amount equal to the appropriate *b*-state energy. Thus, peaks in the spectra resulting from transitions to a given rotational level of the *d* state, e.g., $R(J)$ and $P(J+2)$, occur at the same energy in Fig. 2, the resultant energy scale reflecting the term energy of the *d* state. The spectral simplification resulting from the pumping of single *b*-state levels is evident, with, for the most part, single, resolved *O*, *P*, *R*, and *S* branches occurring in each spectrum.[13] As is the case for the ozone-photolysis-derived spectra of Fig. 1, the spectra in Fig. 2 are significantly power broadened, with apparent line widths of $\sim 7$ cm$^{-1}$ FWHM, making it difficult to determine the smaller predissociation line widths. Of particular interest in Fig. 2(b) is the absence of clearly observable transitions to the $J=12$ and 13 levels of the *d* state. This fact is consistent with the conclusion of Lewis *et al.*[2] that the $d(v=1)$ level suffers a local perturbation by the more strongly predissociated $II\,^1\Pi_g$ valence state, near $J=12$, the resultant state-mixing leading to diminution of the corresponding REMPI signal because of increased competition with predissociation. Transition energies for the rotational branches assigned in Fig. 2 are listed in the first part of Table I.[14]

Rotational terms for $d(v=1)$ were deduced from the transition energies in Table I using the $b(v=0)$ terms implied by the spectroscopic constants of Ref. 11,[15] referred to an energy zero for the $X\,^3\Sigma_g^-(v=0)$ state defined by the Zare Hamiltonian.[16] These $d(v=1)$ terms, for the most part supported by combination differences,[17] are listed in Table II and displayed as reduced terms (circles) in Fig. 3, grouped in segments labeled *a* through *e*. Four local perturbations are evident, culminating at $J\approx 12$, 30, 39.5, and 46, respectively, with effective interaction matrix elements $H_{12}\approx 11$, 18, $\approx 21$, and $\approx 22$ cm$^{-1}$, respectively. Previously, only segment-*a* and some segment-*b* terms have been reported,[2,3,9] containing only the single perturbation at $J\approx 12$, attributed to a homogeneous interaction with the $v=5$ level of the $II\,^1\Pi_g$ valence state.[2] The new perturbations observed here are evidently due to the $v=6$ to 8 levels of the same state. This interpretation is supported by coupled-channel (CC) calculations using the $^1\Pi_g$ Rydberg-valence interaction model of Ref. 2 (solid curves in Fig. 3, raised by 8 cm$^{-1}$), which are in excellent structural agreement with the experimental results. These new experimental data should be useful in refining the CC model of Lewis *et al.*[2]

A quadratic fit to the segment-*a* terms in Table II yields the following spectroscopic constants: $\nu_0=68\,230.4\pm 0.3$ cm$^{-1}$, $B=1.661\pm 0.012$ cm$^{-1}$, and $D=(2.7\pm 0.9)\times 10^{-4}$ cm$^{-1}$, where the uncertainties are $1\sigma$ values and the root-mean-square deviation of the fit is 0.4 cm$^{-1}$. This *B* value is consistent with expectation for a Rydberg series converging on the $v=1$ level of the ionic ground state $X\,^2\Pi_g$ which has $B=1.66$ cm$^{-1}$,[18] the anomalously large *D* value arising because of the perturbation by the valence state discussed above. The present band origin differs by $-8$ cm$^{-1}$ and $+4$ cm$^{-1}$, respectively, from the values reported by Morrill *et al.*,[1] derived from the experiments of Sur *et al.*[9] and Loo,[10] supporting the suggestion in Ref. 1 that those experiments

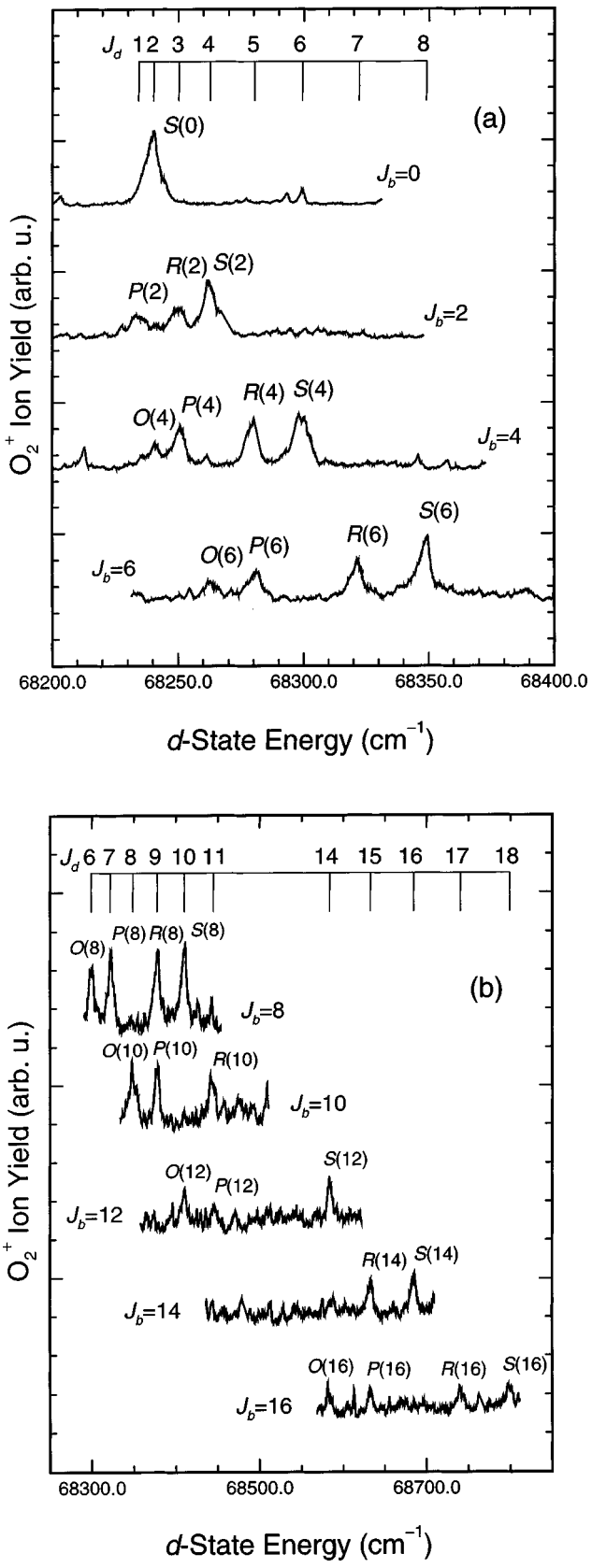


FIG. 2. OODR-[$(1+1')+1'$]-REMPI spectra accessing the $d\,^1\Pi_g(v=1)$ state of $O_2$ via various rotational levels of the $b\,^1\Sigma_g^+(v=0)$ state. (a) $J_b=0-6$. (b) $J_b=8-16$. The spectra have been shifted to higher energy by amounts equal to the appropriate *b*-state energy, the resultant energy scale thus reflecting the term energy of the *d* state, relative to $X\,^3\Sigma_g^-(v=0)$. Some weaker features in the spectra are due to $(2'+1')$ resonances from the *b* state.

TABLE II. Rotational term values for the $d\,^1\Pi_g(v=1)$ level of $O_2$, in $cm^{-1}$, relative to $X\,^3\Sigma_g^-(v=0)$. For $J\leqslant 18$, the terms are from the OODR spectra of Fig. 2; for $J\geqslant 23$, the terms are from the ozone-photolysis-derived spectra of Fig. 1. The terms occur in five segments, *a* through *e* (see text).

| $J$ | $T_a$ | $T_b$ | $T_c$ | $T_d$ | $T_e$ |
|---|---|---|---|---|---|
| 1 | 68 234.3 | | | | |
| 2 | 68 240.3 | | | | |
| 3 | 68 250.3 | | | | |
| 4 | 68 262.8 | | | | |
| 5 | 68 280.4 | | | | |
| 6 | 68 299.4 | | | | |
| 7 | 68 322.2 | | | | |
| 8 | 68 349.0 | | | | |
| 9 | 68 377.9 | | | | |
| 10 | 68 410.1 | | | | |
| 11 | 68 444.6 | | | | |
| 14 | | 68 584.0 | | | |
| 15 | | 68 633.1 | | | |
| 16 | | 68 684.9 | | | |
| 17 | | 68 740.6 | | | |
| 18 | | 68 799.2 | | | |
| 23 | | 69 145.3 | | | |
| 24 | | 69 224.7 | | | |
| 25 | | 69 307.5[a] | | | |
| 26 | | 69 392.4 | | | |
| 27 | | 69 480.4[b] | | | |
| 28 | | 69 571.4 | | | |
| 29 | | 69 664.5 | | | |
| 30 | | 69 745.5[a] | 69 781.8[a] | | |
| 31 | | | 69 874.0 | | |
| 32 | | 69 860.1 | 69 977.5 | | |
| 33 | | | 70 086.3[a] | | |
| 34 | | | 70 197.9 | | |
| 35 | | | 70 313.1 | | |
| 36 | | | 70 432.0 | | |
| 37 | | | 70 551.3[a] | | |
| 38 | | | 70 674.6 | | |
| 39 | | | 70 795.2[a] | | |
| 40 | | | | 70 943.4 | |
| 41 | | | 70 944.2[a] | 71 073.4 | |
| 42 | | | | 71 209.6 | |
| 43 | | | | 71 347.9 | |
| 44 | | | | 71 492.4 | |
| 45 | | | | 71 636.2[a] | |
| 46 | | | | | 71 804.1 |
| 47 | | | | | 71 950.8[a] |
| 49 | | | | | 72 258.2[a] |

[a]Term value derived primarily from shoulders in spectra.
[b]Term value derived from blended lines in spectra.

were probably uncalibrated. The present segment-*a* and -*b* terms exceed those in the thesis of Ref. 3 by an average of 1.9 $cm^{-1}$, within the combined uncertainties, the residual difference probably arising[3] due to differing degrees of power shifting in the two studies.

Rotational distributions for the $b(v=0)$ state formed in reaction (1), shown in Fig. 4, were deduced from the spectra of Fig. 1 by correcting the apparent strengths of the *S*-branch lines for the effects of probe-laser intensity variations, the two-photon rotational line strengths,[19] and, using the CC calculations,[2] the anomalous effects on the electronic part of the strengths caused by the Rydberg-valence interactions. In this procedure, the ionization step in the REMPI process was assumed to be saturated, the relative ion signals deduced

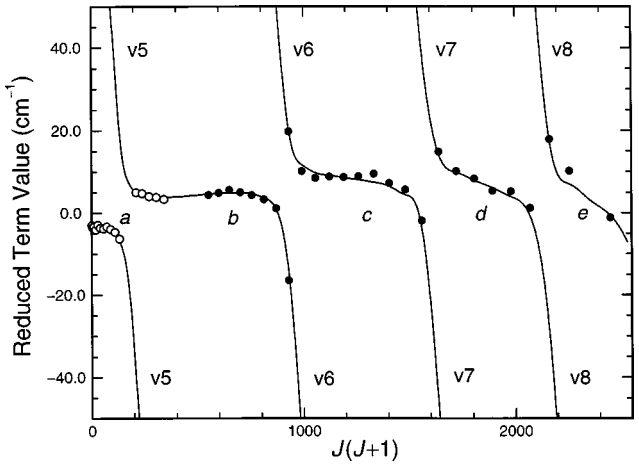


FIG. 3. Comparison between present experimental reduced term values for $d\,^1\Pi_g(v=1)$ (open circles: OODR results, segments *a* and *b*; solid circles: ozone-photolysis-derived results, segments *b* through *e*) and calculations using the CC model of Ref. 2 (solid curves). The computed terms have been raised by 8 $cm^{-1}$. The reduced terms were obtained by subtracting $68\,234 + 1.643J(J+1)$ $cm^{-1}$ from the absolute terms, in order to highlight the perturbations at $J\approx 12$, 30, 39.5, and 46, caused by homogeneous interactions between the Rydberg level $d(v=1)$ and successive levels $v=5$, 6, 7, and 8, respectively (labeled v5, v6, v7, and v8) of the II $^1\Pi_g$ valence state.

from the CC absorption intensities by scaling according to the inverse of the CC predissociation line widths. We emphasize that the present distributions are only roughly determined, with estimated uncertainties near their peaks of $\sim 30\%$. However, it is apparent that the $b(v=0)$-state rotational distributions for photolysis wavelengths of 337.2 and 344 nm, which excite the (4,0,1) and (3,0,1) Huggins bands of $O_3$, respectively,[20] peak near $J=34$ and 28, with FWHMs $\Delta J\approx 15$. A preliminary analysis indicates that excitation of the (3,1,1) band at 340 nm yields a significantly lower $J$ distribution than either of the above. This, apparently vibration-dependent, predissociation thus yields distributions with a much stronger wavelength dependence than predicted by the direct-dissociation model of Levene and Valentini,[21]

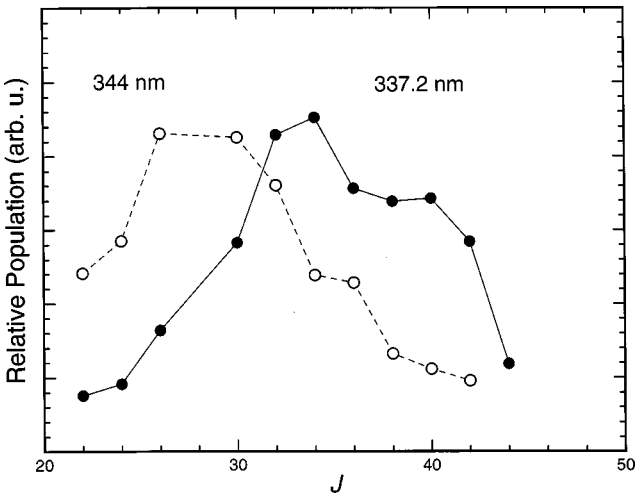


FIG. 4. Rotational-state population distributions for the $O_2[b\,^1\Sigma_g^+(v=0)]$ fragment following photodissociation of $O_3$ at 337.2 and 344 nm, estimated from the *S*-branch spectra of Fig. 1 as described in the text.

and observed in $a(v=0)$-state $J$ distributions following $O_3$ photolysis in the Hartley band.[22] Further investigation of this effect is warranted.


[1] J. S. Morrill, M. L. Ginter, B. R. Lewis, and S. T. Gibson, J. Chem. Phys. **111**, 173 (1999).
[2] B. R. Lewis, S. T. Gibson, J. S. Morrill, and M. L. Ginter, J. Chem. Phys. **111**, 186 (1999).
[3] J. S. Morrill, M. L. Ginter, E. S. Hwang, T. G. Slanger, R. A. Copeland, B. R. Lewis, and S. T. Gibson, J. Mol. Spectrosc. (manuscript in preparation); J. S. Morrill, Ph.D. thesis, University of Maryland (1999).
[4] H. I. Bloemink, R. A. Copeland, and T. G. Slanger, J. Chem. Phys. **109**, 4237 (1998).
[5] P. O'Keeffe, T. Ridley, K. P. Lawley, R. J. Donovan, H. H. Telle, D. C. S. Beddows, and A. G. Urena, J. Chem. Phys. **113**, 2182 (2000).
[6] T. Ridley, K. Lawley, H. Sheard, and R. Donovan, J. Chem. Phys. **116**, 451 (2002).
[7] P. O'Keeffe, T. Ridley, S. Wang, K. P. Lawley, and R. J. Donovan, Chem. Phys. Lett. **298**, 368 (1998).
[8] B. R. Lewis, S. T. Gibson, P. O'Keeffe, T. Ridley, K. P. Lawley, and R. J. Donovan, Phys. Rev. Lett. **86**, 1478 (2001).
[9] A. Sur, R. S. Friedman, and P. J. Miller, J. Chem. Phys. **94**, 1705 (1991).
[10] R. R. Ogorzalek-Loo, Ph.D. thesis, Cornell University, 1989.
[11] L. C. O'Brien, H. Cao, and J. J. O'Brien, J. Mol. Spectrosc. **207**, 99 (2001).
[12] Where possible, the transition energies were averaged over both spectra.
[13] The $Q$-branches are essentially absent, in agreement with expectation for two-photon rotational line strengths in $\Delta\Omega=1$ transitions (Ref. 19).
[14] The listed transition energies do not, of course, include the energy shifts used for display purposes in Fig. 2.
[15] The $b(v=0)$ spectroscopic constants of Ref. 11 are strictly applicable only for $J\leqslant 40$. Thus, our $d$-state terms derived from rotational-branch lines originating from $b(v=0)$-state levels with $J=41-50$ are subject to extrapolation uncertainties. It is likely, however, that these uncertainties are much smaller than the experimental uncertainties.
[16] R. N. Zare, A. L. Schmeltekopf, W. J. Harrop, and D. L. Albritton, J. Mol. Spectrosc. **46**, 37 (1973).
[17] The term values were determined, where possible, as averages of values determined separately from the pairs of lines accessing a given $d$-state level, i.e., $R(J)$ and $P(J+2)$, or $S(J)$ and $O(J+4)$, with the proviso that the result from an unblended line was preferred when the other line of the pair was blended.
[18] R. R. Laher and F. R. Gilmore, J. Phys. Chem. Ref. Data **20**, 685 (1991).
[19] R. G. Bray and R. M. Hochstrasser, Mol. Phys. **31**, 1199 (1976).
[20] P. O'Keeffe, T. Ridley, K. P. Lawley, and R. J. Donovan, J. Chem. Phys. **115**, 9311 (2001; Vibrational quantum numbers refer to symmetric stretch, bend, and asymmetric stretch, respectively.
[21] H. B. Levene and J. J. Valentini, J. Chem. Phys. **87**, 2594 (1987).
[22] J. J. Valentini, D. P. Gerrity, D. L. Phillips, J.-C. Nieh, and K. D. Tabor, J. Chem. Phys. **86**, 6745 (1987).